Automatic Mandible Segmentation on CT Images Using Prior Anatomical Knowledge

Nava Aghdasi[1], Yangming Li[1], Angelique Berens[1], Kris Moe[1]
Blake Hannaford[1]

[1] University of Washington, Seattle WA 98105, USA
{navaa,ymli81,berens,krismoe,blake }@uw.edu

Abstract. We present a fully automatic method for segmenting mandible in CT images using anatomic landmarks and prior knowledge. The aim is to utilize spatial relationship of anatomic landmarks with image processing techniques to detect mandible robustly and efficiently. Applying prior knowledge and reliable anatomical landmarks to define an optimal Region of Interest (ROI) which contains the mandible is an effective way for fast localization and successful segmentation. This approach can be used to segment other structures such as optic nerves by defining a new set of relevant landmarks. This approach is robust to CT data with different scanner setting and does not require large training data sets.

1 Introduction

The primary treatments for head and neck cancer are radiotherapy, surgery and chemotherapy [1]. In the planning stage for the radiotherapy and surgical treatments, clinicians must identify and mark the outline of critical structures on patient images. There are several regions of interest that should be considered in planning that are either therapy targets or critical structures that should be avoided. Although some recent commercial software allows for semi or fully automated segmentation, their application is limited. Manual delineation of structures using drawing tools by a trained expert is commonly used in clinics. This technique is time-consuming and suffers from larger inter- and intra- rater variability. The use of automated image segmentation saves effort, time and increases precision. However, as a result of the image acquisition process, partial volume effect and noise are present in CT images and the poor soft tissue contrast makes the automatic segmentation a difficult problem.

Mandible is one of the structures that must be avoided during the radiation due to presence of mandibular nerves and arteries in this region which have critical roles in patients' health. The challenge in mandible segmentation is due to ambiguous connection of the thin mandibular bones to the upper part of the skull.

Considering similarity in the spatial relation of a structure in human head and relations between different structures, employing prior anatomical knowledge is critical for accurate segmentation [2] [3].

We are interested in developing of an efficient technique for segmenting mandible or other structures by using the anatomical landmarks and prior knowledge. Particularly,

the segmentation is done by combining the anatomical knowledge from clinicians with image processing techniques. For instance, the spatial relation of the mandible to the nasal bone or anterior aspect of the frontal bone in human skull is a beneficial knowledge in segmentation process.

2 Method

The proposed method progressively locates the relevant anatomical landmarks to restrict the original volume to a smaller volume which has a higher probability of containing the desired structure. Multiple sets of landmarks must be defined for various structures due to their different spatial relations in the head. However once defined, they can be used to obtain the specific ROI for each structures in any new data sets.
After finding the smallest volume that contains the desired structure, the segmentation is performed in this smaller volume, which makes the process efficient and accurate.
In the case of the mandible, the segmentation was performed by registration of the mandible models to the obtained volume in order to find the affine transformation. Then labels were transformed to the target volume to segment the mandible. Next, the landmarks and method are described in detail.

2.1 Initial landmarks detection

Limiting the search area to the smallest region that contains the desired structure, decreases the computational time and improves the segmentation precision.
For each structure, ROIs were determined by detecting successive predefined landmarks in bone and tissue thresholded volumes. For instance, the skull base region which separates the brain from other face structures was determined by detecting the nasal tip point and anterior aspect of the frontal bone. For mandible the anterior volume below the skull base was defined as an initial ROI and was obtained by detecting the nasal tip point and ignoring all slices above the landmark [4].
The bone and tissue threshold values were acquired by analyzing the intensity profile of the horizontal mid-line in all axial slices, Figure 1. Due to bones' higher intensity in CT images, the local maximums were detected in the intensity curves. The anatomical knowledge such is distance between two maximums, which reveal the width of the skull, were checked to validate the acquired points. Maximums and the intensity of adjacent points were used as threshold values for the bone and tissue. The obtained threshold values with this approach were independent of scanner's setting.

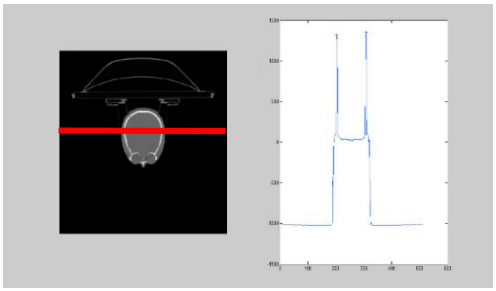

Figure 1. Bone and tissue threshold were obtained by analyzing the intensity profile of the horizontal mid-line

To obtain the described ROI, the nasal tip positions in tissue thresholded volumes was detected with following steps. Initially the volume was cropped at center of the mass to contain only the head and neck structures. Next, the triangulated mesh of the tissue thresholded volume was constructed. The intersection of a 3D vertical line with the mesh was determined as the line moved over a 512×512, x-y grid starting from center. The frontal part of the mesh with no more intersection of the line and mesh was labeled as nasal point, Figure 2.

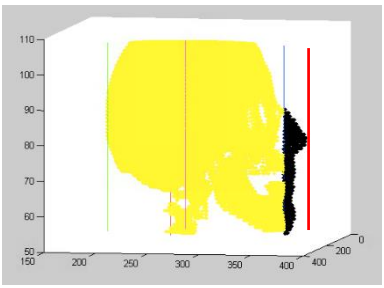

Figure 2. Triangulated mesh of the soft tissue thresholded and vertical line to detect the nasal tip position

In defining the mandible ROI, the nasal tip position was used as a relevant landmark and the volume above that point was ignored in the z direction, which was irrelevant in segmenting the mandible, Figure 3.

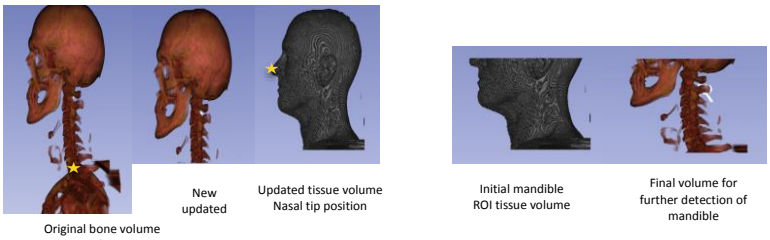

Figure 3. Mandible Initial ROI – left to right: 1) Original bone volume. 2) New volume by cropping the original volume using center of mass. 3) Nasal point position in tissue thresholded volume. 4) Initial mandible ROI. 5) Final volume for mandible.

2.1.2 Updated mandible ROI by registration

The final volume from previous step can be restricted even more to only contain mandible and no other structures such as cervical vertebrae. This was achieved by registration of mandible models to the target volume, obtained from previous step.

Mandible models are 3D point clouds constructed from the mandible ground truth labels. The position of foreground voxels in the binary label volume was used to create the point cloud.

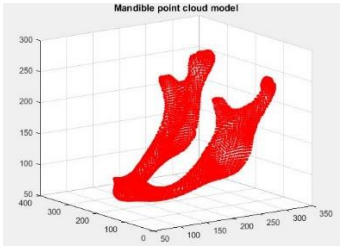

Figure 4. Mandible model point cloud

The target point cloud was constructed from the bone thresholded volume and also with the foreground voxel positions.
Five mandible point cloud models were constructed from the training data. The initial alignment was performed by identifying the translation between the most anterior aspect of the point cloud on models and the target.
For final alignment, the affine transformation was found using the pairwise Iterative Closest Point (ICP) [5]. This step confined the final volume to achieve the initial segmentation. The transformed point cloud was converted to binary volume and only target voxels which overlapped with the mask were labeled as mandible.

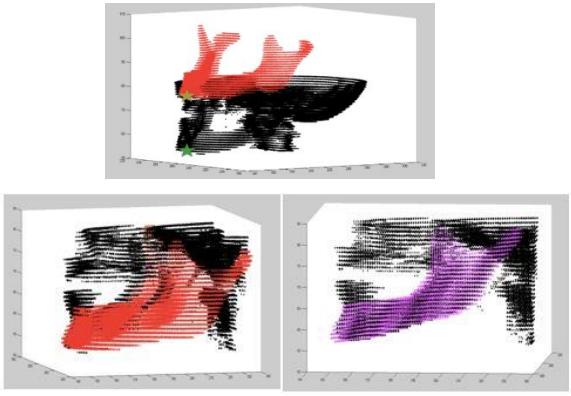

Figure 5. Top – One mandible model and target point cloud. Down – Mandible target and one of the model initially aligned (left), registered target with mandible model (right)

2.2.1 Mandible 2D Refinement

The mandible segmentation was improved by analyzing 2D axial slices. Visual inspection and comparison of 2D slices with the ground truth suggested that there are two cases where the mandible segmentation can be improved.

Case 1: 2D slices where the mandible pixels were not labeled fully, for instance pixels on the edge were not labeled, Figure 6 (left).
Case 2: 2D slices where non mandible pixels was labeled as mandible, Figure 6 (right).
These cases were adjusted, by considering the 2D anatomy of the mandible in axial direction and based on number of objects detected in binary volume which may contain one or multiple objects, Figure7. Each 2D axial slice of the binary volume obtained from affine registration of point cloud can have one or multiple connected objects.
For the binary mask slices with one connected object, the image dilation was used to cover all the mandible pixels in the corresponding slice in target image. Binary mask dilation for these slices improved the mandible segmentation by covering and labeling the pixels on the edge.
For case 2 where the segmented pixels did not belong to mandible, we used a new 2D binary mask. In this case, the new mask was the first slice where mandible binary mask contained two separated objects. The new binary mask was used to segment the mandible pieces for upper slices. Defining a mask for each specific target volume improves the segmentation accuracy for small joint regions of the mandible.

Figure 6. Left – case 1: 2D slices where the mandible pixels were not labeled fully. Right – case 2: 2D slices where non mandible pixels was labeled as mandible.

Figure 7. 2D anatomy of the mandible in axial direction which may contain one or multiple individual objects.

3 Results and discussion

The training data sets comprised 33 patient CT data from the Radiation Therapy Oncology Group, with ground truth segmentation of mandible and some other structures such as optic nerve. The segmentation was stored as binary masks for assessment and visualization. Additional 10 patients CT data were provided for testing.

The reconstruction matrix for all datasets was 512×512 pixels with (0.98~1.16) × (0.98~1.16) pixel size and (2 ~ 3) mm slice thickness.
The Hausdorff distance and volumetric overlap (Dice metric) were used as criteria in axial slice for quantitative comparison of results from proposed method and ground truth. Table 1, summarize the evaluation results according to these two main criteria.
The average dice coefficient for mandible was 0.7 which is considered to be a good segmentation. This results can be improved by changing the number of iterations and error threshold in ICP registration
The method was used to segment the optic nerves by using the anatomical knowledge and defining a new set of landmarks. For segmenting optic nerves, the volume between the nasal and frontal bone was used as initial ROI. Based on visual review, the segmented optic nerves were wider than ground truth however they had similar shapes, Figure 9. Also for many cases, the superior and inferior rectus muscles were labeled as optic nerves. These issues produced a low dice coefficient result for optic nerves which can be improved in future work.

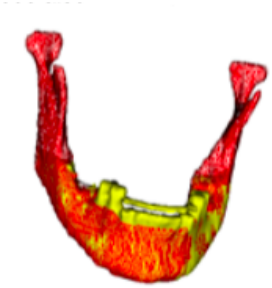

Figure 8. Mandible segmentation: Yellow – ground truth, Red – segmentation results

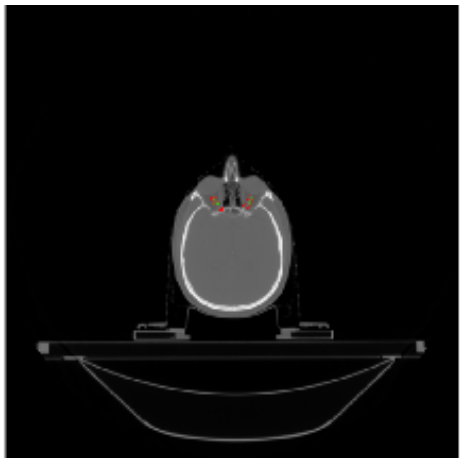

Figure 9. Optic nerves segmentation – axial slice: Green – ground truth, Red – segmentation results

Dataset No	Mean Dice			Mean HD		
	Optic Nerve		Mandible	Optic Nerve		Mandible
	Left	Right		Left	Right	
1	0.4197	0.1477	0.9043	3.2478	7.0373	5.2119
2	0.4172	0.3743	0.7868	5.5233	5.6088	17.23
3	0.3886	0.3760	0.7999	4.755	8.4499	13.144
4	0.2956	0.0813	0.7330	11.184	9.492	24.4913
5	0.2292	0.3017	0.7978	7.3127	6.3399	19.1556
7	0.5256	0.3819	0.8053	3.3326	6.3280	5.7706
8	0.2986	0.3007	0.8430	10.939	6.2857	7.5
9	0.4520	0.3481	0.8386	10.212	6.592	4.990
10	0.4742	0.1759	0.7621	9.276	15.540	16.921
11	0.3064	0.3387	0.8413	11.781	8.3051	6.733
12	0.0028	0.2516	0.7209	10.174	6.0761	20.523
13	0.4370	0.3008	0.6965	5.4202	11.554	11.27
14	0.4263	0.4362	0.7402	10.109	8.1765	8.6476
15	0.4975	0.4273	0.7517	10.860	5.9298	5.1390
Mean	0.3447	0.2828	0.7833	8.3613	8.4254	13.0791

Table 1. Mean dice and Hausdroff for mandible and optic nerves

4 Conclusion

In this paper we have presented a fully automatic knowledge based segmentation pipeline to segment the mandible and optic nerves from CT images on a public dataset. This method utilizes the anatomic landmarks to restrict the original volume to smaller volume and segment the desired structures in the smaller volumes. The mandible results were good and can be improved by improving the ICP results and adding post-segmentation processing. Based on visual inspection, optic nerves were segmented wider than ground truth. Therefore, additional image processing operations can be used for precise segmentation. This method was efficient, did not required many training data sets and produced reasonable segmentation for new data sets. The method appears robust to image artifacts caused by metal within the teeth and successfully detects landmarks in the image even with presence of medical equipment required for patient treatment.

5 References

1. Haffty, B.G., Wilson L.D.: Handbook of Radiation Oncology: Basic Principles and Clinical Protocols. Jones & Bartlett Learning (2008)
2. Kobashi, Masaharu, and Linda G. Shapiro. "Knowledge-based organ identification from CT images." Pattern Recognition 28.4 (1995): 475-491.
3. Teng, Chia-Chi, Linda G. Shapiro, and Ira Kalet. "Automatic segmentation of neck CT images." Computer-Based Medical Systems, 2006. CBMS 2006. 19th IEEE International Symposium on. IEEE, 2006.
4. Milap, P., Mehta, Julian, D. Perry: Medial Orbital Wall Landmarks in Three Dif- ferent North American Populations. Orbit. 34,72–78 (2015).
5. Kroon, Dirk-Jan. Segmentation of the mandibular canal in cone-beam CT data. University of Twente [Host], 2011.